Geophys. Astrophys. Fluid Dynamics, Vol. 65, pp. 127–147
Reprints available directly from the publisher
Photocopying permitted by license only

CONDUIT SOLITARY WAVES IN A VISCO-ELASTIC MEDIUM

ROGER H. J. GRIMSHAW

School of Mathematics, The University of New South Wales, Kensington, New South Wales, Australia 2033

KARL R. HELFRICH and J. A. WHITEHEAD

Woods Hole Oceanographic Institution, Woods Hole, MA 02543

(*Received 1 May 1991; in final form 2 January 1992*)

The theory for waves on a buoyant fluid conduit in a more viscous outer fluid is extended to include a visco-elastic outer fluid. The external fluid is treated as a linear Kelvin-type visco-elastic medium and a wave evolution equation is derived. This equation is identical to the purely viscous case with the exception of a new term representing the elastic effects. A conservation law is derived and used in an analytic treatment for a slowly-varying solitary wave (given initially by the exact solution to the purely viscous case) for the case of small, but non-zero, elasticity. The theory shows that the wave amplitude will decay and a shelf, required for the conservation of mass, will develop behind the wave. Numerical solutions of the evolution equation support the analytic approximation. Laboratory experiments show qualitative agreement with the analytic and numerical development. Geophysical applications suggest that these effects may be most important for melt migration in the asthenosphere.

KEY WORDS: Conduits, solitary waves, visco-elastic fluids.

1. INTRODUCTION

In recent years there has been considerable interest in the dynamics of buoyant viscous diapirs and conduits in a more viscous fluid. A main application of these studies has been to geophysics. Buoyant, low viscosity zones are thought to exist in the Earth's mantle as a result of heating, say at the core-mantle boundary, or as a result of partial melting in the upper mantle. Rayleigh-Taylor instability then causes the formation of diapirs and trailing conduits (Whitehead and Luther, 1975). Applications to geophysical phenomena such as the formation and evolution of mantle plumes and swells, flood basalts, hot spots, melt migration in the upper mantle and magma chamber replenishment have recently been reviewed by Olson (1990) and Whitehead and Helfrich (1990). Schubert *et al.* (1989) have shown that these ideas apply to cartesian plumes in fluids with temperature dependent viscosity.

One of the interesting aspects of these studies is that buoyant low viscosity conduits can support nonlinear solitary waves (Scott *et al.*, 1986; Olson and Christenson, 1986; Helfrich and Whitehead, 1990). Numerical calculations and laboratory experiments show that the waves are remarkably stable and are nearly preserved upon collision. Furthermore, the solitary waves contain closed streamlines and therefore transport isolated parcels of fluid over significant distances. This property

may be important in the transport of isolated deep mantle material to the base of the lithosphere (Whitehead and Helfrich, 1988).

Over the long times associated with mantle convection and the extreme pressures deep in the mantle, the mantle is usually considered a viscous fluid. However, under certain circumstances the mantle behaves as a non-Newtonian fluid. In particular, over time scales of $O(10^4$–10^{11} s) (the visco-elastic relaxation time) the mantle behaves as a visco-elastic fluid (Turcotte and Schubert, 1982). Although these times are short compared to typical mantle time scales, if a solitary conduit wave propagates a significant fraction of its wavelength over a time of $O(10^{11}$ s) or less, then elasticity may become important. For a large solitary wave with wavelength λ and phase speed c the time scale Δt of wave passage is (Olsen, 1990)

$$\Delta t = \frac{\lambda}{c} = \left(\frac{8\nu_2}{g'c}\right)^{1/2}. \tag{1.1}$$

Here ν_2 is the kinematic viscosity of the outer fluid, $g' = g(\rho_2 - \rho_1)/\rho_1$ is the reduced gravity, g is the acceleration due to gravity and ρ_1 (ρ_2) is the density of the inner (outer) fluid. Following Whitehead and Helfrich (1988) and Olsen (1990) typical values for the mantle are $c = 5 \times 10^{-9}$ m s^{-1}, $g' = 0.1$ m s^{-2} and $\nu_2 = 10^{17}$ m^2 s^{-1}. With these values (1.1) gives $\Delta t = O(10^{13}$ s).

This value is two orders of magnitude greater than the upper bound of $O(10^{11}$ s) that Turcotte and Schubert (1982) suggest for elastic effects to be significant. Thus one might expect elasticity to be relatively unimportant. However, mantle rheology is not directly observed on those time scales. The estimates could easily be incorrect by several orders of magnitude and verification could only come from direct observation. In addition, over propagation distances that are long with respect to a wavelength, the cumulative effects of even weak elasticity may become significant. For example, solitary waves might be affected during transit from the core-mantle boundary to the mantle-crust interface. Also, the above time scale is for passage of an entire wave, but deformation is also occurring on faster time scales. Since conduit waves may play an important role in mantle heat and mass transfer it is worthwhile to see how the waves would be affected by this simple non-Newtonian rheology.

Another possible application concerns mixing in magma chambers. It is well known that viscosity of magma increases with silica content due to polymerization of the silica. Thus a condition could be found where conduits are formed which contain solitary waves whose presence would greatly alter the mixing between ambient and intrusive magmas. It is possible that such materials also become elastic from the presence of the polymers or from suspended crystals. In that case, solitary waves might be strongly effected by the elastic properties of the host material.

A third possible application arises because conduits (and conduit waves) have also been shown to be simple analogs of compaction driven porous flow of melt in a viscous matrix (Scott *et al.*, 1986). The area of the conduit is analogous to the melt volume fraction (porosity) and the outer fluid is analogous to the viscous matrix. Movements of melt in the upper mantle typically occur on shorter time scales than deep mantle motions. Scott and Stevenson (1986) estimate a time scale for melt

movement as magmons (analogous to conduit solitary waves) of 3×10^{11} s. Visco-elastic effects may well be important in that regime. Analysis of the conduit problem should provide some insight into the dynamics of upper mantle melt migration.

Studies of visco-elastic fluid processes have been extensively conducted in chemical engineering, but few studies have been conducted in geophysical fluid dynamics. However, the mantle of the earth (and presumably of other terrestial planets) has both elastic and fluid behavior. Thus problems involving visco-elastic behavior are particularly relevant to mantle dynamics. We consider this study to be a first approach to this area.

In Section 2 the viscous conduit theory is modified to take into account visco-elastic behavior and a wave evolution equation is derived. The outer fluid is treated as a Kelvin-type visco-elastic medium in which total stress is given by the sum of the elastic stress and the viscous stress. In Section 3 analytical and numerical solutions on the slow modulation of a solitary wave by weak elasticity are given. Laboratory experiments which are used to qualitatively test the theory are presented in Section 4. A discussion of the results and possible geophysical applications are contained in Section 5.

2. DERIVATION OF THE EVOLUTION EQUATION

The theoretical model we adopt consists of a viscous fluid which in the undisturbed state occupies a vertical cylindrical pipe of radius a, surrounded by an infinite visco-elastic medium which we shall assume is denser, much more viscous and endowed with an elastic property which tends to resist the deformation of the pipe radius. Since the derivation of the governing equation is analogous to the non-elastic case described by Scott *et al.* (1986), Olson and Christenson (1986) and Helfrich and Whitehead (1990), we shall only sketch the derivation here.

We choose non-dimensional co-ordinates for which the length scale is the undisturbed pipe radius a, the velocity scale is $U = g(\rho_2 - \rho_1)a^2/4\mu_1$, and the time scale is a/U. Here ρ_1 (ρ_2) is the density of the inner (outer) medium and μ_1 is the dynamic viscosity of the inner fluid. The dynamic pressure (i.e., the pressure relative to the hydrostatic pressure in the outer medium) is scaled by $\mu_1 U/a$. With this scaling the Reynolds number is

$$R = \frac{\rho_1 a U}{\mu_1} = \frac{g\rho_1(\rho_2 - \rho_1)a^3}{4\mu_1^2}. \tag{2.1}$$

We adopt cylindrical polar co-ordinates in which x is aligned along the (vertical) pipe axis, and r is the radial co-ordinate (see Figure 1). Then we seek axisymmetric solutions in which the deformed pipe radius is given by $\eta(x,t)$. Assuming that a typical deformation of the pipe radius is associated with an axial wavenumber α, we can make analytical progress by assuming that $\alpha R \ll 1$, and $\alpha^2 \ll 1$. In this solution the flow in the pipe is just Poiseuille flow to leading order, and the dimensionless

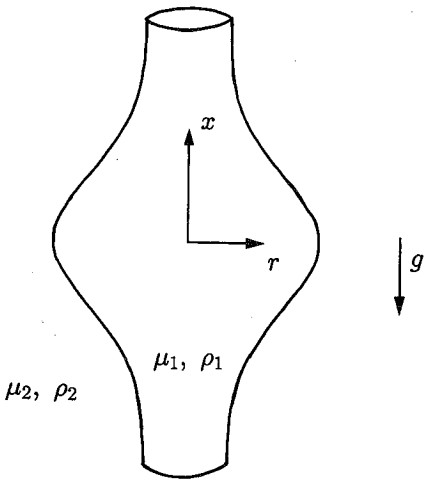

Figure 1 The coordinate system.

pressure deviation from hydrostatic pressure p and axial velocity u in the inner fluid are approximately given by

$$p = B, \tag{2.2a}$$

$$u = (1 - \tfrac{1}{4}B_x)(\eta^2 - r^2) + C. \tag{2.2b}$$

Here B and C are functions of x and t, which are determined from the boundary conditions at the interface with the outer medium. Conservation of mass within the pipe gives the equation [using (2.2b)]

$$\eta\eta_t + \{(1 - \tfrac{1}{4}B_x)\tfrac{1}{4}\eta^4 + \tfrac{1}{2}C\eta^2\}_x = 0. \tag{2.3}$$

In the outer medium we assume that the viscosity is $\mu_2 = m\mu_1$ where $m \gg 1$; indeed, we assume that $m\alpha^2$ scales with unity. It then follows that the dynamic pressure p and axial velocity u in the outer medium are $O(m^{-1})$ and to leading order can be ignored. In particular, continuity of u at the interface $r = \eta$ then implies that C in (2.2b) is $O(m^{-1})$, and can likewise be ignored. Next the radial velocity v in the outer medium is given to leading order by

$$v = Dr^{-1}, \qquad r > \eta, \tag{2.4}$$

where D is a function of x and t. This result follows most easily from convervation of mass in the outer medium. Further, the kinematic condition at the interface shows that to leading order

$$D = \eta\eta_t. \tag{2.5}$$

It remains to impose the conditions for continuity of the normal and tangential stresses at the interface. The condition arising from the continuity of the tangential stress is not needed here, and hence we consider only the normal stress condition which to leading order is

$$B=\frac{2mD}{\eta^2}+\gamma\eta. \tag{2.6}$$

Here the first term on the right-hand side arises from the viscous normal stress term $2mv_r$ in the outer medium evaluated at $r=\eta$, and we have used (2.4) to determine v_r. The second term is that due to the elasticity in the outer medium, and arises from the simple hypothesis that there is an elastic pressure in the outer medium which is proportional to the pipe radius. This is true for a thick hollow elastic cylinder, whose change in inner radius r' corresponding to an excess pressure p' is given by [Popov, 1952 (p. 418)]

$$r'=\frac{1+\sigma}{E}r_i p',$$

where E is Young's Modulus, σ is Poisson's ratio and r_i is the initial inner radius. Since in dimensional variables the proportionality constant between r' and p' is $E/r_i(1+\sigma)$, then in our present non-dimensional co-ordinates

$$\gamma=RE/\rho_1 U^2(1+\sigma). \tag{2.7}$$

This hypothesis is essentially equivalent to taking the outer fluid to be a linear Kelvin visco-elastic material (Turcotte and Schubert, 1982). One might want to picture the conduit sheathed by a thin elastic pipe surrounded by a viscous fluid. We choose this model, rather than a Maxwell-type material, for mathematical simplicity. This assumption is discussed further in Section 5. We note in passing that if interfacial surface tension is taken into account then an extra term $\delta\eta^{-1}$ would appear on the right-hand side of (2.6), where $\delta=S/\mu_1 U$ and S is the surface tension coefficient. Whereas we shall show in the next section that the elastic term is stabilizing (i.e., leads to damping), it can similarly be shown that this surface-tension term is destabilizing (i.e., leads to growth).

Finally with B given by (2.6), and setting C equal to zero in (2.3), we obtain the desired evolution equation which is

$$\eta\eta_t+\left\{\left(1-\tfrac{1}{4}\left[\frac{2m\eta_t}{\eta}+\gamma\eta\right]_x\right)\tfrac{1}{4}\eta^4\right\}_x=0. \tag{2.8}$$

Here, we have used (2.5) to determine D in (2.6).

3. ANALYTICAL AND NUMERICAL SOLUTIONS

The equation to be studied is thus (2.8). It is convenient to make the following transformations

$$A=\eta^2 \tag{3.1a}$$

and

$$T=\frac{2t}{\sqrt{m}}, \qquad X=\frac{2x}{\sqrt{m}}. \tag{3.1b}$$

Note that (3.1b) is consistent with the long-wave approximation already used (viz. $\alpha^2 \ll 1$ with $m\alpha^2$ being a quantity which scales with unity), and A is proportional to the cross-sectional area of the pipe. Then (2.8) becomes

$$A_T+\left\{\left(1-\left[\frac{A_T}{A}+\varepsilon\sqrt{A}\right]_X\right)\tfrac{1}{2}A^2\right\}_X=0, \tag{3.2a}$$

$$\varepsilon=\frac{\gamma}{2\sqrt{m}}. \tag{3.2b}$$

We shall base our discussion on the hypothesis that ε is a small parameter, but defer until Section 5 any consideration of likely physical values for ε.

When $\varepsilon=0$ equation (3.2a) has Olson and Christenson's (1986) solitary wave solution given by

$$A=A_0(\theta), \tag{3.3a}$$

where

$$\theta=X-cT \tag{3.3b}$$

and

$$cA_{0\theta}^2=2c(A_0-1)^2-2A_0^2\ln A_0+(A_0^2-1). \tag{3.3c}$$

Note that the condition $A_0\to 1$ as $|\theta|\to\theta$ has been used in deriving (3.3c). In terms of the maximum wave amplitude A_m, the speed c is given by

$$c=\frac{2A_m^2\ln A_m-(A_m^2-1)}{2(A_m-1)^2}. \tag{3.4}$$

From this expression it can be shown that $c>1$ for all $A_m>1$, is a monotonically

increasing function of A_m, and $c \to 1$ as $A_m \to 0$. These waves have a typical Gaussian shape and at low amplitudes are given by

$$A_0 = 1 + (A_m - 1)\,\mathrm{sech}^2\,\beta\theta + \mathrm{O}(A_m - 1)^2, \tag{3.5a}$$

where

$$c - 1 = \tfrac{1}{3}(A_m - 1) + \mathrm{O}(A_m - 1)^2, \tag{3.5b}$$

and

$$A_m - 1 = 6\beta^2. \tag{3.5c}$$

For large amplitudes,

$$A_0 \approx 1 + A_m \exp(-\beta^2\theta^2), \tag{3.6a}$$

where

$$c \approx \ln A_m - \tfrac{1}{2}, \tag{3.6b}$$

and

$$2c\beta^2 \approx 1. \tag{3.6c}$$

Helfrich and Whitehead (1990) have shown numerically that these waves are extremely stable, and tend to preserve their shapes after interactions. Indeed their behavior is almost soliton-like in that the interactions produce only a very small amount of radiating oscillations.

Here we show that the effect of the elasticity of the outer medium, represented here by the ε-term, is to cause these waves to decay. A typical numerical solution is shown in Figure 2. Note that associated with the wave decay is the production of a trailing shelf which is visible as a slight elevation behind the wave. This is to be expected as these solitary waves have only a single degree of freedom, say the speed c in terms of which the amplitude A_m and the width, β^{-1}, are completely determined. Hence as the wave amplitude decays the wave mass decreases, so fluid is deposited behind the wave in the conduit as a trailing shelf. The situation is analogous to that for the solitary wave solutions of the perturbed KdV equation (see Johnson, 1973 or Grimshaw, 1979). Indeed, in the weakly nonlinear limit, Whitehead and Helfrich (1986) have shown that (3.2a) with $\varepsilon = 0$ can be reduced to a KdV equation, and the same analysis with $\varepsilon \neq 0$ will obviously produce a perturbed KdV equation.

We shall quantify these observations by two complementary approaches for the case when ε is a small, but non-zero, parameter. First we consider the implications of two conservation laws for equation (3.2a). The first of these is just (3.2a) itself and represents the conservation of mass. The second is obtained by multiplying (3.2a)

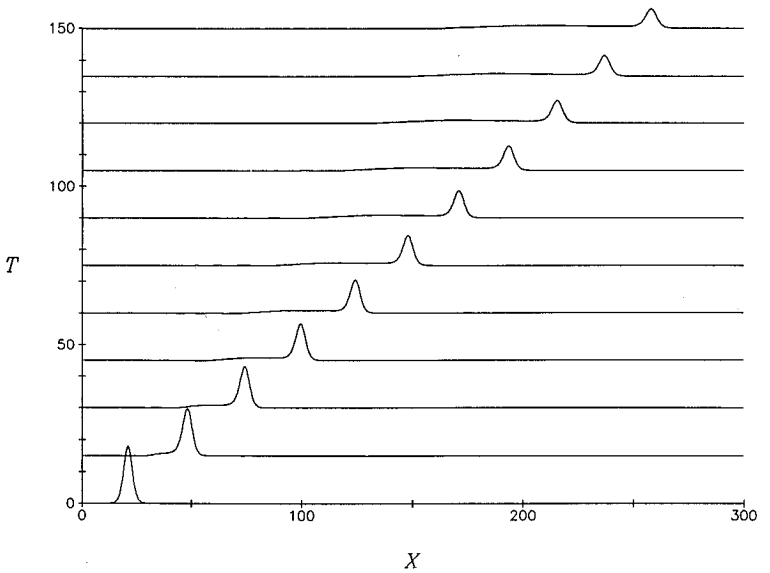

Figure 2 Numerical solution of (3.2a) with $\varepsilon=0.2$ and an initial condition of a solidary wave [given by (3.3c)] with $A_m=5.0$. The numerical method is that used by Helfrich and Whitehead (1990).

by A^{-2} and subtracting (3.2a) from the result. We then get

$$E_T+F_X+\varepsilon G=0, \tag{3.7a}$$

where

$$E=\frac{(A-1)^2}{A}+\tfrac{1}{2}\frac{A_X^2}{A^2}, \tag{3.7b}$$

$$F=\tfrac{1}{2}(A^2-1)-\ln A-\tfrac{1}{2}(A^2-1)\left(\frac{A_T}{A}\right)_X, \tag{3.7c}$$

and

$$G=\left(\frac{1}{A^2}-1\right)[\tfrac{1}{2}A^2(\sqrt{A})_X]_X. \tag{3.7d}$$

Strictly speaking this is not a true conservation law as the εG-term cannot be written as a flux. The physical interpretation of (3.7a) is not immediately evident, but it is analogous to a conservation law discovered by Barcilon and Richter (1986) for an equation similar to (3.2a). We shall call (3.7a) the equation for conservation of "energy" since in the weakly nonlinear limit E is quadratic in $(A-1)$.

To proceed, we now propose that (3.2a) has a slowly.varying solitary wave solution given by

$$A = A_0(\theta, \tau) + \varepsilon A_1(\theta, \tau) + \ldots, \tag{3.8a}$$

where

$$\theta = X - \frac{1}{\varepsilon}\int_0^\tau c(\tau')\,d\tau', \tag{3.8b}$$

and

$$\tau = \varepsilon T. \tag{3.8c}$$

Here τ is a slow time variable; a slow spatial variable εX could also be used but for simplicity is omitted here. A_0 is given by (3.3a,c) where the speed $c(\tau)$ is now slowly-varying and hence (3.3b) is replaced by (3.8b). To obtain the behavior of $c(\tau)$, and hence that of the amplitude $A_m(\tau)$ [see (3.4)], we use the conservation law (3.7a). Expressing this in terms of θ and τ, and integrating over θ we find that

$$\frac{\partial E_0}{\partial \tau} + G_0 = 0, \tag{3.9a}$$

where

$$E_0 = \int_{-\infty}^{\infty} \left\{ \frac{(A_o - 1)^2}{A_0} + \tfrac{1}{2}\frac{A_{0\theta}^2}{A_0^2} \right\} d\theta, \tag{3.9b}$$

and

$$G_0 = \int_{-\infty}^{\infty} \left\{ \tfrac{1}{2}\frac{A_{0\theta}^2}{A_0^2}\sqrt{A_0} \right\} d\theta. \tag{3.9c}$$

In deriving the expression for G_0 we have integrated by parts. Since both E_0 and G_0 are clearly positive, equation (3.9a) shows that the wave amplitude must decay. Note that, using (3.3c), it can be shown that

$$E_0 = \int_{-\infty}^{\infty} \left\{ (A_0 - 1) - \frac{1}{c}\ln A_0 \right\} d\theta, \tag{3.10a}$$

and

$$F_0 = cE_0,$$

where F_0 is the corresponding flux term obtained from (3.7c). Indeed if a slow spatial variable $\xi = \varepsilon X$ is included, then (3.9a) is replaced by

$$\frac{\partial E_0}{\partial \tau} + \frac{\partial}{\partial \xi}(cE_0) + G_0 = 0. \tag{3.11}$$

At this point it may be queried why the conservation law (3.7a) has been used in preference to (3.2a). We shall show below that a direct calculation of A_1, leads to (3.9a), thus justifying our choice. First, however, we give a more intuitive explanation. We anticipate that as the solitary wave deforms a trailing shelf is formed whose amplitude scales with ε, and which extends horizontally over a distance ε^{-1}. Hence the mass [i.e., $(A-1)$] of this shelf scales with unity and is comparable to the mass of the solitary wave itself. Thus the conservation law (3.2a) cannot be used on the wave alone. However, the "energy" E of the shelf scales with ε becaue E is quadratic in $(A-1)$ [see (3.7b)]. Hence, to leading order, we can use (3.7a) applied to the wave alone, and the outcome is (3.9a). Returning to the mass conservation law (3.2a) let us now suppose that the amplitude of the trailing shelf at the rear of the solitary wave is A_1^-. Then, integrating (3.2a) over the wave we readily deduce that

$$(c-1)A_1^- = -\frac{\partial}{\partial \tau} \int_{-\infty}^{\infty} (A_0 - 1)\, d\theta. \tag{3.12}$$

Since here the solitary wave is decaying, the right-hand is positive, and hence the trailing shelf is one of elevation.

To conclude, we now return to the perturbation expansion (3.8a) and consider the equation for A_1, which is

$$-cA_{1\theta} + \frac{\partial}{\partial \theta}\left\{A_1 A_0\left[1 + c\left(\frac{A_{0\theta}}{A_0}\right)_\theta\right] + \tfrac{1}{2}cA_0^2\left(\frac{A_1}{A_0}\right)_{\theta\theta}\right\} + F_1 = 0, \tag{3.13a}$$

where

$$F_1 = A_{0\tau} - \frac{\partial}{\partial \theta}\left\{\tfrac{1}{2}A_0^2 \frac{\partial}{\partial \theta}\left(\frac{A_{0\tau}}{A_0} + \sqrt{A_0}\right)\right\}. \tag{3.13b}$$

Equation (3.13a) can be integrated once with respect to θ, assuming that $A_1 \to 0$ as $\theta \to \infty$ ahead of the solitary wave, but note that we are anticipating that $A_1 \to A_1^-$

which is not necessarily zero as $\theta \to -\infty$ at the rear of the solitary wave. Thus we get

$$-cA_1 + A_1 A_0 \left[1 + c\left(\frac{A_{0\theta}}{A_0}\right)_\theta\right] + \tfrac{1}{2}cA_0^2\left(\frac{A_1}{A_0}\right)_{\theta\theta} + G_1 = 0, \tag{3.14a}$$

where

$$G_1 = -\int_\theta^\infty F_1 \, d\theta'. \tag{3.14b}$$

Equation (3.14a) is a linear second order ordinary differential equation for A_1, where the homogeneous part is the linearization of the corresponding equation for A_0, which is not explicitly shown here but can be obtained by differentiation of (3.3c). Since this equation for A_0 is invariant with respect to phase shifts in θ, it follows that $A_{0\theta}$ is a solution of the homogeneous part of the equation A_1. Given this, we can solve (3.14a) for A_1. We shall not give details as the main result is the following compatibility condition which is necessary and sufficient for A_1 to be bounded with respect to θ,

$$\int_{-\infty}^{\infty} G_1 \frac{A_{0\theta}}{A_0^3} d\theta = 0, \tag{3.15a}$$

or

$$\int_{-\infty}^{\infty} F_1\left(1 - \frac{1}{A_0^2}\right) d\theta = 0. \tag{3.15b}$$

Substitution of (3.13b) into (3.15b) determines the variation of $c(\tau)$. It can now be demonstrated that (3.15b) is equivalent to (3.9a). Further, letting $\theta \to -\infty$ in (3.14a) we can recover the result (3.12) for the trailing shelf.

It remains to use (3.9a) to determine the predicted rate of decay for $c(\tau)$ [or $A(\tau)$ through (3.4)]. Unfortunately, because an exact analytical formula for $A_0(\theta)$ cannot be obtained from (3.3c), we are unable to find analytical formulas for E_0 and G_0 as functions of θ (or equivalently as functions of A_m). However, the approximate formulas (3.6a–c) can be used to deduce that for large amplitudes,

$$2A_m(\ln A_m)^2 \approx (\tau_0 - \tau)^2 \tag{3.16}$$

where τ_0 is a constant. Similarly, the approximate formulas (3.5a–c) can be used to deduce that for small amplitudes,

$$A_m - 1 \approx 45/2(\tau_0 + \tau). \tag{3.17}$$

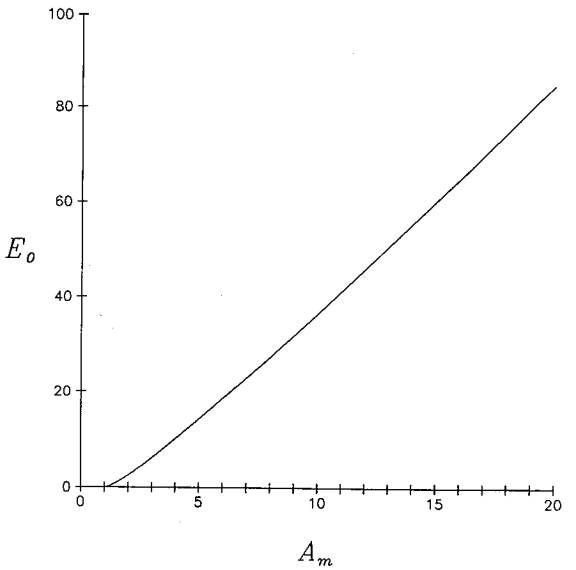

Figure 3 E_0 given by (3.10a) as a function of A_m.

For arbitary amplitudes numerical solutions were used to obtain $A_m(\tau)$ [or $c(\tau)$]. First (3.10a) and (3.9c) can be combined with (3.3c) and (3.4) to calculate $E_0(A_m)$ and $G_0(A_m)$. These functions are shown in Figures 3 and 4, respectively. Next, (3.9a) can be rearranged and integrated once to give

$$\tau - \tau_0 = -\int \frac{dE_0}{dA_m}\frac{1}{G_0} dA_m. \tag{3.18}$$

This equation can be integrated numerically using the previously calculated functions $E_0(A_m)$ and $G_0(A_m)$. The resulting relationship between A_m and τ is shown in Figure 5. Note that an arbitary constant has been added to $\tau = \varepsilon T$. The time to decay from A_{m1} to A_{m2} is

$$\tau = \tau(A_{m2}) - \tau(A_{m1}). \tag{3.19}$$

From Figure 5 we can find that the time (or distance) for one-half amplitude decay decreases as A_{m1} or ε increases (recall that $\tau = \varepsilon T$). Large waves decay more rapidly than smaller waves and the decay rate increases as the elasticity of the outer fluid increases.

Wave decay determined by numerical solutions of the full wave equation (3.2a) was compared to the predictions of the slowly-varying theory (Figure 5). Figure 6 shows the results of this comparison for initial wave amplitude $A_{m1} = 5.0$ and several values of ε. Figure 7 shows the same except for $A_{m1} = 10.0$. The slowly-varying approximation agrees reasonably well with the full numerical solutions, with the

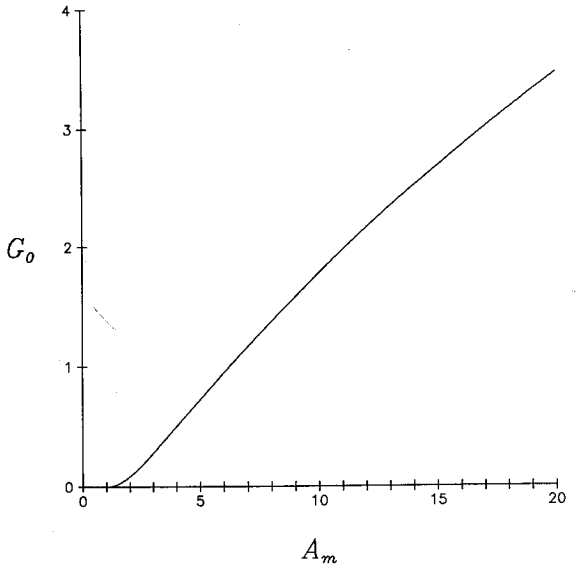

Figure 4 G_0 given by (3.9c) as a function of A_m.

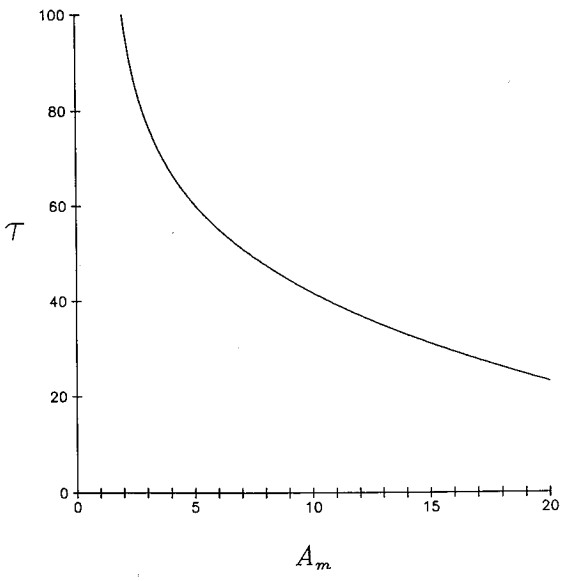

Figure 5 Half amplitude decay time τ from (3.18) as a function of A_m.

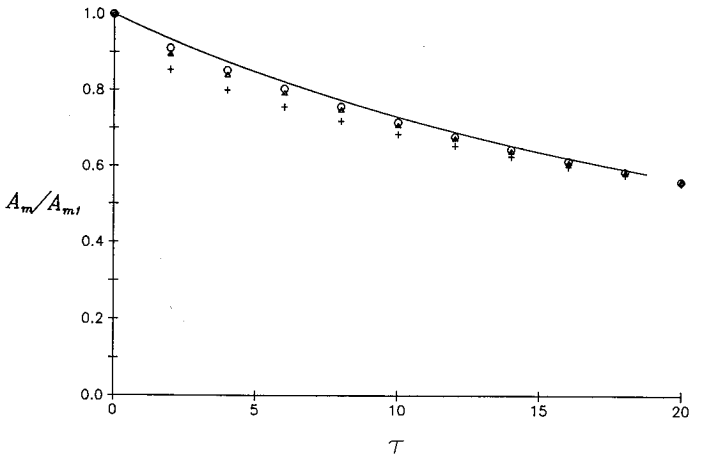

Figure 6 Comparison of the slowly-varying approximation (3.18) (——) and numerical solutions of wave decay using (3.2a) for $A_{m1}=5.0$ and $\varepsilon=0.0707$ (○); 0.1414 (Δ); 0.3535 (+).

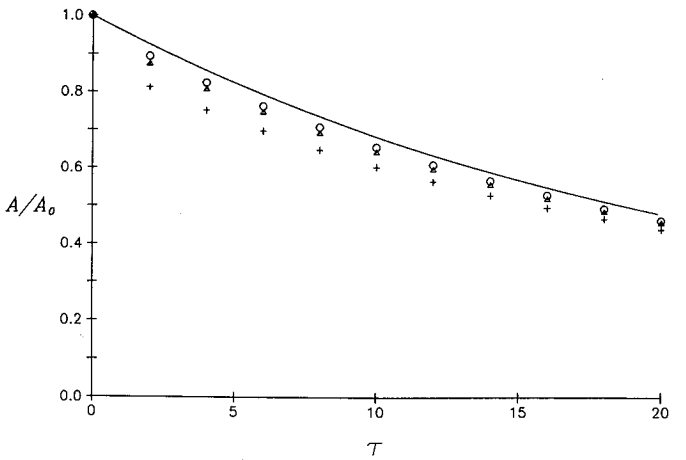

Figure 7 Same as Figure 6 except $A_{m1}=10.0$.

approximation predicting slightly smaller decay. The agreement improves as A_{m1} or ε is decreased and as τ increases.

4. EXPERIMENTS

Laboratory experiments were conducted to test the qualitative predictions of the theoretical and numerical work. The method follows that used by Helfrich and Whitehead (1990) where solitary waves were observed in conduits of a water-syrup

mixture in syrup. The essential difference here is that the outer fluid, although much more viscous than the inner fluid, is also slightly elastic. The experiments were conducted in a cylindrical column of 7.6 cm diameter filled to a height of 40 cm with a visco-elastic fluid (see below). The buoyant intrusive fluid was introduced through a vertical steel tube of 0.17 cm inside diameter positioned over the center of the tank bottom. Intrusive fluid was fed from a reservoir with a constant head to creat a steady vertical conduit. Waves on the conduit were produced by injecting a volume of intrusive fluid from a syringe into the feeder system. The previous work by Helfrich and Whitehead (1990) showed that one solitary wave of the type given by (3.3c) will develop rapidly, within several wave lengths from the tube. The intrusive fluid was dyed for visualization and side view photographs were taken. The photographs were used to extract quantitative information on wave evolution.

The inner fluid was a 70:30 mixture by volume of Karo brand light corn syrup and water. At 23°C this mixture has viscosity $\mu_1 = 0.40 \pm 0.04\,\mathrm{gm\,cm^{-1}\,s^{-1}}$ and density $\rho_1 = 1.257\,\mathrm{gm\,cm^{-3}}$ (Helfrich and Whitehead, 1990). The outer fluid was a 4:1 mixture of Karo corn syrup and 1% solution by weight of carboxymethylcellulose (CMC) and water. CMC is a commercially available polymer which when mixed with water gives a viscous fluid with elastic properties (Aqualon Company, 1989). CMC solutions have complicated rheologies, but do show typical visco-elastic characteristics such as partial recovery after strain (a feature of Maxwell fluids) and the phenomenon of rod climb. Both the viscosity and the elasticity of the solution increase as the weight fraction of CMC is increased. At 25°C a 1% CMC solution has a viscosity of approximately $28\,\mathrm{gm\,cm^{-1}\,s^{-1}}$ which decreases as the strain rate increases (Aqualon Company, 1989). However, the shear stress is linear with strain rate for 0.5% CMC solution in water for strain rates less than $10\,\mathrm{s^{-1}}$. Our experimental rates are significantly less than this, so non-Newtonian behavior is limited to elastic rather than more complicated behavior such as a power law relation between stress and strain. The mixture of 1% CMC solution and corn syrup gives a fluid with $\mu_2 = 30 - 40\,\mathrm{gm\,cm^{-1}\,s^{-1}}$, $\rho_2 = 1.34\,\mathrm{gm\,cm^{-3}}$ and weak but observable elastic behavior. This gives $m = \mu_2/\mu_1 = 75 - 100$. We estimate the visco-elastic relaxation time to be 1–2 s. This was determined by observing the relaxation after the cessation of an applied strain. Precise measurement of the rheological properties of the visco-elastic outer fluid was not possible with our available laboratory equipment. Therefore quantitative comparison of the theory and experiment was not possible, but qualitative behavior can be examined.

Figure 8 shows side view photographs of solitary wave evolution in a visco-elastic outer fluid. Figure 8a shows the wave shortly after emerging from the injection tube. In Figure 8b the same wave is shown 48 s later when it is 14.1 cm further up the conduit. Figure 8c is the same wave 88 s after, and 24.6 cm above, the wave in Figure 8a. There is noticeable wave decay with distance. The amplitude has decayed by a factor of 0.69 from Figure 8a to 8c. The photographs show that the conduit behind the wave is slightly bigger than the conduit ahead of the wave, indicating the presence of a trailing shelf. In Figures 8a, b and c the ratio of conduit area ahead of the wave to the area 2–3 wavelengths behind the wave is 0.73 ± 0.02.

Figure 9 shows photographs of solitary waves produced by injecting dyed conduit

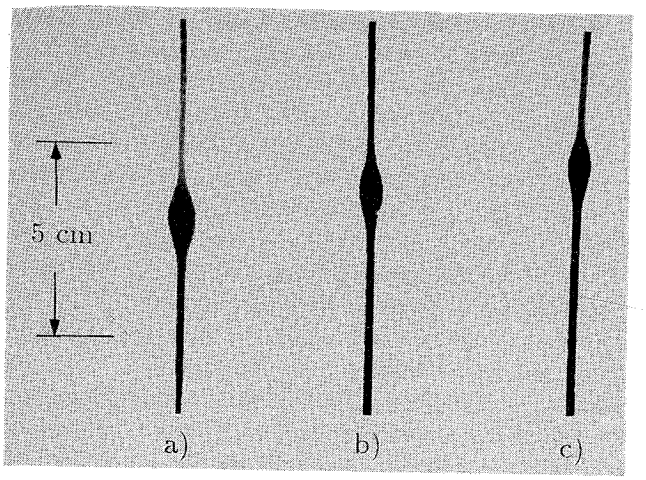

Figure 8 Photographs of solitary wave evolution along the conduit. The horizontal lines are separated by 5 cm. (a) A Solitary wave shortly after emerging from feeder tube. (b) Same wave 48 s after and 14.1 cm above (a). (c) Same wave 88 s after and 24.5 cm above (a).

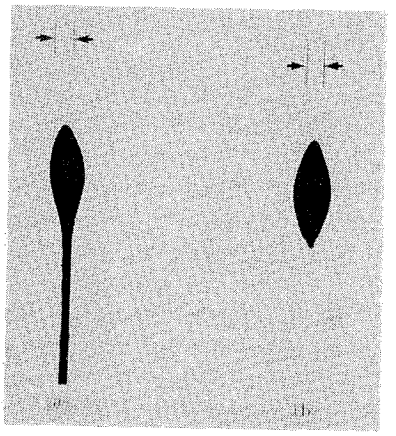

Figure 9 Photographs of dyed fluid in a clear conduit that is being carried by a solitary wave. When the outer fluid is visco-elastic (a), dyed fluid is deposited behind the wave at the center of the conduit. This forms the "shelf" that forms as the result of wave decay. For a Newtonian outer fluid (b), no fluid is deposited behind the wave. The arrows define the clear conduit ahead of the waves.

fluid into a colorless conduit. With the visco-elastic outer fluid (Figure 9a) dyed material which makes up the wave is continuously deposited behind the wave in the center of the conduit. With a Newtonian outer fluid (pure corn syrup) (Figure 9b) no material is left behind. These photos show that in the case of a visco-elastic outer fluid the trailing shelf that develops behind the decaying wave is formed from conduit fluid which leaks from the parcel of fluid that is transported with the wave. A

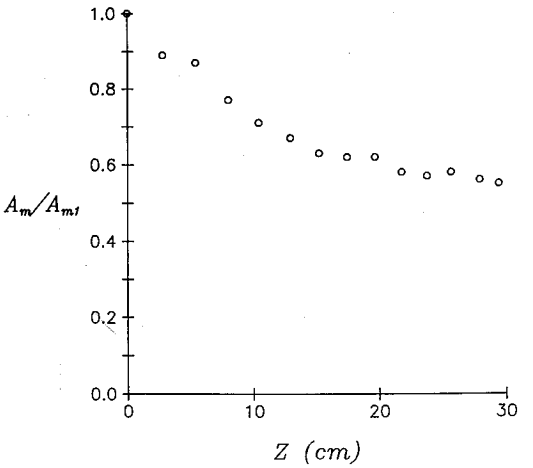

Figure 10 Plot of wave measured amplitude A_m normalized by initial amplitude A_{m1} as a function of distance along the conduit x. Here $A_{m1}=9.9$.

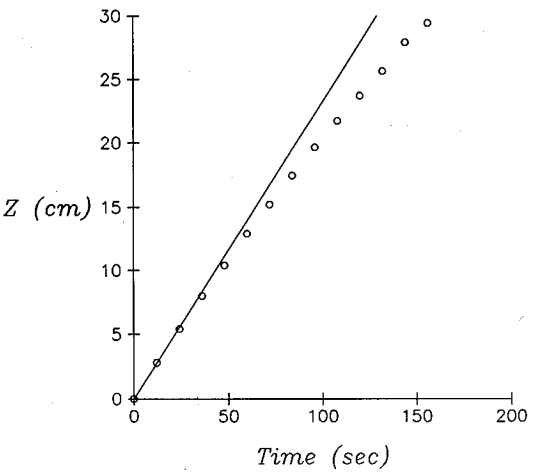

Figure 11 Plot of wave position x versus time t for the run shown in Figure 10. Also shown is a solid line which corresponds to a constant phase speed calculated from the first two data points.

Newtonian outer fluid leads to closed streamlines within the wave and no leakage (cf., Helfrich and Whitehead, 1990).

In Figure 10 the maximum measured wave area (amplitude) A_m, normalized by the initial wave amplitude A_{m1}, is plotted as a function of distance up the conduit from an experiment with $A_{m1}=9.9$ (normalized with the initial conduit area). The data show a clear trend of amplitude decay. Figure 11 shows the wave position x versus time t for the run in Figure 10. Also shown is a straight line which corresponds

to a constant phase speed calculated from the first two data points. There is continuous decrease of phase speed, consistent with the reduction in amplitude shown in Figure 10.

The propagation distances are large with respect to the initial solitary wave half-width (≈ 0.5 cm). If we take $m=75$ and the initial measured conduit radius $a=0.073$ cm (3.1b) gives $X=44.6$ and 77.3 for Figures 8b and 8c respectively. From Figures 8 and 11 we estimate a length scale $\lambda \approx 0.5$ cm and an average phase speed $c \approx 0.3$ cm s^{-1}. This gives a wave passage time scale $\Delta t = \lambda/c \approx 1.7$ s. Given our estimate of 1–2 s for the visco-elastic time scale, we have that the ratio of visco-elastic to propagation time scales is ≈ 1. The effects of elasticity are important, but do not dominate viscous effects.

Other runs with different initial amplitudes and conduit diameters showed the same behavior. In experiments with a purely viscous outer fluid Helfrich and Whitehead (1990) found no measureable reduction in wave amplitudes and constant phase speeds over propagation distances a number of times longer than those considered here. The effects observed in these experiments are certainly due to a visco-elastic affect from the presence CMC in the outer fluid. The observations of wave amplitude decay, phase speed reduction and the formation of a trailing shelf are all consistent with the predictions of the theoretical and numerical work.

5. DISCUSSION

The theory and experiments show that a visco-elastic outer fluid results in wave damping. As a solitary wave decays a shelf is formed behind the wave. Fluid is continually squeezed out of the wave and deposited along the conduit centerline. The volume of expelled fluid is proportional to the amplitude reduction since the volume anomaly of a wave is directly proportional to A_m (for $A_m \gg 1$). This contrasts with the purely viscous case in which solitary waves have closed streamlines and transport isolated parcels of fluid (Whitehead and Helfrich, 1988).

The relevance of these results to geophysics depends upon ε, the elastic parameter, and the distance the wave travels. Figure 5 shows that a wave with initial amplitude $A_m=10$ decays by one-half in $\tau=\varepsilon T \approx 20$. The dimensional one-half decay time is

$$t_{1/2} \approx \frac{40}{\varepsilon} \frac{\mu_1 m^{1/2}}{g' a \rho_1}, \tag{5.1}$$

where, from (2.7) and (3.2b),

$$\varepsilon = \frac{2E}{g' m^{1/2} a \rho_1 (1+\sigma)}. \tag{5.2}$$

For typical antle values $m=10^4$, $\mu_1 = 3\times 10^{16}$ kg m^{-1} s^{-1}, $g'=0.1$ m^2 s^{-1}, $\rho_1 = 3\times 10^3$ kg m^{-3} and $a=10^4$ m we find from (5.1),

$$t_{1/2} \approx \frac{1}{\varepsilon} 10^6 \text{ yr}. \tag{5.3}$$

Taking $E=10^{11}$ Pa and $\sigma=0.3$, (5.2) gives $\varepsilon\approx 5\times 10^{2}$. This value of ε is extremely large and (5.3) gives unrealistically short damping times of $O(10^3$ yr).

The reason for the short damping times lies in the choice of the Kelvin-type model for visco-elastic behavior. This model does not allow viscous stress relaxation, so that large elastic stresses can be generated even for very low strain rates. In the wave equation (3.2a) the ratio of elastic to viscous influence in the external fluid is given by the ratio of the two terms in the square brackets,

$$\delta=\varepsilon\frac{A^{3/2}}{A_T}. \tag{5.4}$$

Taking the value of ε given above, a wave amplitude $A=10$, and the corresponding time scale for solitary wave passage, $\Delta T=1$, we find $\delta=O(10^3)$. The elastic stress is much larger than viscous stress, which is not true for the deep mantle on long time scales.

A more appropriate model for geophysical applications is thought to be the Maxwell fluid (Turcotte and Schubert, 1982) which does permit stress relaxation. However, the wave equation (3.2b) did a good job of describing wave behavior. The theory predicted amplitude and phase speed decay along with formation of a trailing shelf, all observed in the experiments. The mixture of corn syrup and CMC solution does permit stress relaxation and to first order might be considered a Maxwell fluid. Thus, some insight into wave damping in a Maxwell fluid is gained from this simpler Kelvin model.

A crude assessment of wave decay in geosphysical conditions may be made with this model if a more realistic estimate for the elastic parameter ε can be obtained. In a Maxwell medium the ratio of elastic to viscous effects is given by

$$\delta_M=\frac{2\mu_2}{Et_s}, \tag{5.5}$$

where t_s is the time scale of change of strain (i.e., wave passage). The quantity $2\mu_2/E$ is the visco-elastic relaxation time discussed in Section 1. Equating the ratios of elastic to viscous effects from the two models [(5.4) and (5.5)] we get an estimate for ε,

$$\varepsilon=\frac{\delta_M}{A^{1/2}\Delta T}. \tag{5.6}$$

We can test this scaling with the laboratory experiments. For the experiments $\delta_M\approx 1$. Now, for the run shown in Figures 10 and 11, $A_{m1}=9.9$ and $\Delta T=1$, which gives $\varepsilon\approx 0.3$ from (5.6). Taking $\mu_1=0.40\,\text{gm cm}^{-1}\,\text{s}^{-1}$, $\rho_1=1.257\,\text{gm cm}^{-3}$, $m=75$, $\rho_2=1.34\,\text{gm cm}^{-3}$, $g=980\,\text{cm s}^{-2}$, and $a=0.07$ cm we have from (5.1) that $t_{1/2}\approx 80$ s. From Figures 10 and 11, the wave decays to $A_m/A_{m1}=0.56$ in $y\approx 160$ s. The data do not extend to a decay of one-half, but extrapolation gives $t_{1/2}\approx 200$ s. The ad-hoc scaling gives a decay time that is within a factor of two to three of the observed

value. Although the above analysis is crude we can apply the scaling to construct order-of-magnitude estimates for geophysical systems. The goals are not precise estimates, but rather explorations of possible relevance.

For deep mantle conditions we have previously estimated that $\delta_M = O(10^{-2})$, which gives $\varepsilon \approx 3 \times 10^{-3}$ for $A = 10$ and $\Delta T = 1$. From (5.3) $t_{1/2} \approx 300$ Ma. For a wave with phase speed $c = 5 \times 10^{-9}\,\mathrm{m\,s^{-1}}$ this corresponds to a decay distance $x_{1/2} \approx 5 \times 10^{7}$ m. This is much greater than the mantle depth, therefore visco-elastic damping, as we have already noted, is not likely to be important for conduit waves propagating from the deep mantle. However, there are a number of uncertainties that argue against making a direct application at this stage. First, as mentioned in the introduction, the deep mantle rheology is not well known for the time scales of interest so the conclusions may change. Second, no detailed knowledge of actual solitary waves in the mantle exist at present. Third, the argument developed here is only approximate at best.

In the upper mantle, where melt migration may occur by porous flow, the analogy between the compaction problem and the conduit problem can be exploited to estimate the effect of damping of magmons. Here $t_s \approx 10^{11}$ s (Scott and Stevenson, 1986) giving $\delta_M = O(1)$. Again taking $A = 10$ and $\Delta T = 1$ we get from (5.4) that $\varepsilon \approx 1$, which gives $t_{1/2} \approx 3 \times 10^{13}$ s. Taking a velocity scale for magmons of $3 \times 10^{-9}\,\mathrm{m\,s^{-1}}$ (Scott and Stevenson, 1986) we get $x_{1/2} \approx 100$ km. This distance is consistent with estimates of the depth in which porous flow of melt may occur (Scott and Stevenson, 1986). Magmons will experience a reduction of their maximum porosity as they propagate vertically through the matrix and higher melt concentrations will be left behind the magmon.

Of course, other effects such as melting (Fowler, 1990), or two- and three-dimensional effects [since the conduit analogy is for one-dimensional porous flow [Scott *et al.*, 1986)] may alter these conclusions. Furthermore, the estimates were based upon an ad-hoc equivalence of ratios of elastic to viscous effects for two different rheological models. Correct analysis of the conduit problem, or the complete porous flow problem, with a more realistic constitutive relation is necessary. The present model was chosen for mathematical simplicity and to provide insight into the physics. Incorporation of even the linear Maxwell model greatly complicates the present problem. However, it does appear possible that visco-elastic rheology could influence melt migration in the upper mantle.

Acknowledgements

RHJG was supported for a visit to the Woods Hole Oceanographic Institution by the Center for Coastal Studies. KRH and JAW are supported by National Science Foundation Grant EAR-8916857. Robert Frazel helped with the experiments and photography. Woods Hole Oceanographic Institution Contribution No. 7676.

References

Aqualon Company, *Aqualon Cellulose Gum, Sodium Carboxymethylcellulose: Physical and Chemical Properties*, Aqualon Co., Wilmington, DE, 19850–5417 (1989).

Barcilon, V. and Richter, F. M., "Nonlinear waves in compacting media," *J. Fluid Mech.* **164,** 429–448 (1986).

Fowler, A. C., "A compaction model for melt transport in the Earth's asthenosphere. Part II: Applications," in : *Magma Transport and Storage* (Ed. M. P. Ryan), John Wiley and Sons (1990).

Grimshaw, R. "Slowly varying solitary waves I. Korteweg-de Vries equation," *Proc. R. Soc. Lond.* A **368,** 359–375 (1979).

Helfrich, K. R. and Whitehead, J. A., "Solitary waves on conduits of buoyant fluid in a more viscous fluid," *Geophys. Astrophys. Fluid Dynam.* **51,** 35–52 (1990).

Johnson, R. S., "On an asymptotic solution of the Korteweg-de Vries equation with slowly varying coefficients," *J. Fluid Mech.* **60,** 813–824 (1973).

Olson, P., "Hot spots, swells and mantle plumes," in: *Magma Transport and Storage* (Ed. M. P. Ryan) John Wiley and Sons (1990).

Olson, P. and Christenson, U., "Solitary wave propagation in a fluid conduit within a viscous matrix," *J. Geophys. Res.* **91(B),** 6367–6374 (1986).

Popov, E. P., *Mechanics of Materials*, Prentice-Hall, Englewood Cliffs, N.J., 441pp (1952).

Schubert, G., Olsen, P., Anderson, C. and Goldman, P., "Solitary waves in mantle plumes," *J. Geophys. Res.* **94,** 9523–9532 (1989).

Scott, D. R. and Stevenson, D. J., "Magma ascent by porous flow," *J. Geophys. Res.* **91(B),** 9283–9296 (1986).

Scott, D. R., Stevenson, D. J. and Whitehead, J. A., "Observations of solitary waves in a viscosity deformable pipe," *Nature* **319,** 759–761 (1986).

Turcotte, D. L. and Schubert, G. *Geodynamics*, John Wiley and Sons, New York (1982).

Whitehead, J. A. and Helfrich, K. R., "The Korteweg-de Vries equatin from laboratory conduit and magma migration equations," *Geophys. Res. Lett.* **13,** 545–546 (1986).

Whitehead, J. A. and Helfrich, K. R., "Wave transport of deep mantle material," *Nature* **336,** 59–61 (1988).

Whitehead, J. A. and Helfrich, K. R., "Magma waves and diapiric dynamics," in: *Magma Transport and Storage* (Ed. M. P. Ryan) John Wiley and Sons (1990).

Whitehead, J. A. and Luther, D. S., "Dynamics of laboratory diapir and plume models," *J. Geophys. Res.* **80,** 705–717 (1975).

GEOPHYSICAL AND ASTROPHYSICAL FLUID DYNAMICS

GENERAL INFORMATION

AIMS AND SCOPE

Geophysical and Astrophysical Fluid Dynamics exists for the publication of original research papers and short communications, occasional survey articles and conference reports on the fluid mechanics of the earth and planets, including oceans, atmospheres and interiors, and the fluid mechanics of the sun, stars and other astrophysical objects. In addition, their magnetohydrodynamic behaviors are investigated. Experimental, theoretical and numerical studies of rotating, stratified and converging fluids of general interest to geophysicists and astrophysicists appear. Properly interpreted observational results are also published. Notes for contributors can be found at the back of the journal.

ORDERING INFORMATION
Four issues per volume. 1992 Volume(s): 65–69.
Orders may be placed with your usual supplier or directly with Gordon and Breach Science Publishers S.A., c/o STBS Ltd (distributor for Gordon and Breach Science Publishers S.A.), P.O. Box 90, Reading, Berkshire RG1 8JL, UK or PO Box 786, Cooper Station, New York, NY 10276, USA. Journal subscriptions are sold on a volume basis only; single issues of the current volume are not available separately. Claims for nonreceipt of issues should be made within three months of publication of the issue or they will not be honored free of charge. Subscriptions are available for microform editions. Details will be furnished upon request.

Subscription Rates: Base list subscription price per volume: ECU 274 (US$256; Dfl 639).* Available only to single users whose library already subscribes to the journal OR who warrant that the journal is for their own use and provide a home address for mailing. Orders must be sent directly to STBS and payment must be made by personal check or credit card.

Separate rates exist for different users such as academic and corporate institutions. These rates may also include photocopy license and postage and handling charges. Special discounts are also available to continuing subscribers through our Subscriber Incentive Plan (SIP).
*The European Currency Unit (ECU) is the worldwide base list currency rate; payment can be made by draft drawn on ECU currency in the amount shown. Alternatively, the US Dollar rate applies only to North American subscribers; The Dutch Guilder rate applies only to